The spliceosome inhibitors isoginkgetin and pladienolide B induce ATF3-dependent cell death in mouse embryonic fibroblasts

Erin J. Vanzyl[1] , Alex B. Blackmore[1] , Hadil Sayed[1] , Kayleigh R.C. Rick[1], Pasan Fernando[1] and Bruce C. McKay[1,2*]

[1] Department of Biology, Carleton University, Ottawa, ON, Canada

[2]Institute of Biochemistry, Carleton University, Ottawa, ON, Canada

[*] Corresponding author

Email: bruce_mckay@carleton.ca

Abstract

The spliceosome assembles on pre-mRNA in a stepwise manner through five successive pre-spliceosome complexes. The spliceosome functions to remove introns from pre-mRNAs to generate mature mRNAs that encode functional proteins. Many small molecule inhibitors of the spliceosome have been identified and they are cytotoxic. However, little is known about the mechanisms leading to cell death. Activating transcription factor 3 (ATF3) is a transcription factor that can stimulate apoptotic cell death in response to a variety of cellular stresses. Here, ATF3 protein levels increased in cultured human and mouse cells in response to cytotoxic levels of the two splicing inhibitors tested: pladienolide B (PB) and isoginkgetin (IGG), that target different pre-spliceosome complexes. Importantly, deletion of ATF3 protected mouse embryonic fibroblasts to these splicing inhibitors. Our results indicate that both splicing inhibitors activate ATF3, and that ATF3 is contributing to the sensitivity of MEFs to these compounds.

Introduction

Most protein-coding genes are transcribed into a precursor RNA (pre-mRNA) that requires significant processing to produce mature mRNA. One of the more complex modifications is the removal of introns and ligation of exons through the process of pre-mRNA splicing. The major spliceosome is responsible for the removal of the vast majority of introns, so it is usually referred to as the spliceosome[1]. The spliceosome is composed of five small nuclear RNAs (snRNAs), U1, U2, U4, U5 and U6, which are each associated with specific proteins yielding their corresponding small nuclear ribonuclear protein complexes (snRNPs). These snRNPs bind sequentially to *cis*-acting elements in pre-mRNA including the 5' and 3' splice

42 sites, the branch sequence, and polypyrimidine tract, leading to the assembly of a functional
43 spliceosome through the E, A, B, B* and C pre-spliceosome complexes[2].
44 A variety of small molecules interfere with the spliceosome at distinct points in assembly.
45 PB is a spliceosome inhibitor derived from *Streptomyces platensis* that targets the SF3B1
46 protein. This protein is a component of the U2 snRNP complex so PB prevents the formation of
47 the A complex[3]. IGG is a natural compound derived from *Ginkgo biloba,* that affects the
48 spliceosome at a subsequent step, preventing the transition from the A to the B complex by
49 inhibiting the stable binding of the U4/U5/U6 tri-snRNP complex[4]. These two compounds
50 affect a different stage of spliceosome formation, however both have been shown to decrease cell
51 viability through uncharacterized mechanisms [5, 6].
52 Activating transcription factor 3 (ATF3) is a member of the ATF/CREB transcription
53 factor family and is activated in response to a variety of stresses including DNA damage,
54 inflammation, endoplasmic reticulum (ER) stress and oxidative stress [7-10]. ATF3 has been
55 shown to have a variety of functions, one of which is regulating the expression of proapoptotic
56 genes, such as GADD153/CHOP[11]. We sought to determine if ATF3 plays a role in sensitivity
57 to the inhibition of pre-mRNA splicing. Here we report that ATF3 is induced in human and
58 mouse cells and that deletion of ATF3 in mouse embryonic fibroblasts (MEFs) protects cells
59 from the lethal effects of spliceosome inhibitors. This work provides important insight into the
60 mechanisms underlying the cell death induced by spliceosome dysfunction.
61

62 # Materials and Methods

63 ## Cell culture and drug treatment

64 HCT116 cells were obtained from the American Tissue Type Collection (Cat #: CCL-247,
65 Manassas, VA) grown in McCoys media (Hyclone, San Angelo) supplemented with 10% Fetal
66 Calf Serum (FBS) (Gibco, Dun Laoghaire) and 90units/ml penicillin, 90ug/ml streptomycin
67 (Hyclone). $ATF3^{+/+}$ and $ATF3^{-/-}$ MEFs were obtained from Dr. Jim Dimitroulakos (Ottawa
68 Hospital Research Institute)(St. Germain *et al.,* 2010) and grown in DMEM High Glucose media
69 (Hyclone) supplemented with 10% Fetal Calf Serum (FBS) (Gibco) and 90units/ml penicillin,
70 90ug/ml streptomycin (Hyclone). Cell were seeded at a density of 500,000 cells/ 6cm or 25,000
71 cells per well of a 96-well plate, 24 hours prior to treatment, depending on the assay. Cells were
72 treated with up to 30µM IGG (Calbiochem), up to 25nM PB (ChemCruz), 200nM actinomycin
73 D (AD) (Sigma-Aldrich, St. Louis, MO), an equivalent volume of dimethyl sulfoxide (DMSO)
74 as the vehicle control for IGG or left untreated.
75

76 # Immunoblotting

77 Cell monolayers were rinsed with phosphate buffered saline (PBS) pH 7.6 and collected in 300µl
78 of 1% SDS in dH_2O. Samples were sonicated (QSonic, Newton), and protein was quantified
79 using the Bio-Rad Protein Assay (Bio-Rad, Philadelphia). Equal amounts of protein were
80 denatured in NuPAGE™ LDS Sample Buffer and NuPAGE™ Sample Reducing Agent (10X)
81 (Fisher Scientific, Ottawa), heated for 10 minutes at 70˚C and loaded onto NuPAGE 4-12% Bis-
82 Tris gels (Fisher Scientific). Protein was then transferred to a nitrocellulose membrane (Bio-
83 Rad), and transferred proteins were stained using 1mg/ml Ponceau S Red in 1% glacial acetic
84 acid. Membranes were blocked for 30-60 minutes in 5% Milk in Tris Buffered Saline Tween
85 (TBST) pH 7.6 (Tris Buffered Saline, 0.1% Tween 20). Membranes were incubated overnight at
86 4˚C in primary antibody, anti-ATF-3 (sc-188, Santa Cruz, CA) or anti-beta-actin (A2228, Sigma)

87 in 0.5% Milk in TBST pH 7.6. Membranes were washed 4x5 min in TBST, then incubated in
88 secondary antibody (HRP-conjugated goat anti-mouse or goat anti-rabbit from Abcam) for 1-2
89 hours. Membranes were washed 4x5 min in TBST, then incubated for 5 minutes in 600µl of
90 Clarity™ Western ECL substrate (Bio-Rad), and imaged using the Fusion FX5 gel
91 documentation system (Vilber Lourmat, France).
92

93 Flow cytometry

94 Floating and adherent cells were collected together by centrifugation following trypsin treatment.
95 The supernatant was removed, and the cell pellet was washed twice in PBS, fixed in 1ml ice cold
96 70% ethanol and stored at -20˚C for a minimum of 30 minutes. Cells were centrifuged, ethanol
97 was then removed, and the pellet was washed twice in PBS and resuspended in 200µl of 20µM
98 Propidium Iodide (PI) stain (Sigma-Aldrich) with 73µM RNaseA (Fisher Scientific). Red
99 fluorescence was measured with a BD Accuri C6 flow cytometer and analyzed using the BD
100 Accuri C6 software.
101

102 Cell viability assays

103 $ATF3^{+/+}$ and $ATF3^{-/-}$ MEFs were seeded in a 96-well plate 24h hours prior to treatment for both
104 cell viability assays. The CellTiter-Glo® Luminescent Cell Viability Assay (Promega, Madison)
105 was used according to manufacturer's instructions to determine ATP content, to estimate cell
106 viability. Briefly, 100µl of media was removed from each well and mixed with an equal volume
107 of CellTiter-Glo Reagent. After 2 minutes of shaking, the samples were incubated at room
108 temperature for 10 minutes and read using the Cytation 5 96 well plate reader (BioTek, Vermont)
109 and Gen5 software (version 2.07.17) at an integration time of 1.0 s per well.

110 For trypan blue dye exclusion assays, cells were detached using trypsin and 10 ul of trypan blue
111 (0.4% in PBS) was added to each well of the 96-well plate. After two minutes, an aliquot of cells
112 was transferred to Dual-Chamber cell counting slides (Bio-Rad, Hercules) and read using the
113 Biorad TC20 Automated Cell Counter.
114

115 Results

116 Splicing inhibitors induce apoptosis and increase ATF3

117 Pre-mRNA splicing is essential for viability and pre-mRNA splicing inhibitors are
118 cytotoxic through an unknown mechanism. To start to address this, HCT116 colon cancer cells
119 were exposed to either IGG or PB and 48 hours later apoptosis was assessed by flow cytometric
120 analysis of subdiploid (subG1) DNA content (Figs 1A and B). Exposure to either splicing
121 inhibitor resulted in an increase in the fraction of cells with sub G_1 DNA content. ATF3 is
122 important in multiple cell death pathways [7, 11, 12] but its role in response to splicing inhibition
123 was unknown. Therefore, we measured the expression of ATF3 in response to treatment with
124 both splicing inhibitors in these cells (Fig 1C). ATF3 levels increased following treatment with
125 cytotoxic concentrations of both splicing inhibitors but the fold increase in ATF3 appears to be
126 greater in PB-treated cells.
127

128 **Fig 1. Increased apoptotic cell population in response to IGG and PB treatment.** HCT116
129 cells were left untreated, exposed to 30μM IGG (A) or 25nM PB (B) for 48 hours (B). Flow
130 cytometric analysis was performed to determine the proportion of cells with sub G_1 DNA content
131 (apoptotic). Each point represented the mean, +/- the standard error of the mean (SEM) from
132 least three independent experiments. (C) protein lysates were collected for HCT116 cells in 1%

133 SDS following 24h untreated, or treated with DMSO, 30μM IGG or 25nM PB, and analyzed
134 using immunoblotting with the indicated antibodies. Similar results were obtained in three
135 independent experiments.
136

137 # ATF3 contributes to cell sensitivity

138 We used a genetic approach to determine if ATF3 contributed to cell death following
139 spliceosome inhibition in isogenic MEF strains that either expressed or did not express ATF3
140 ($ATF3^{+/+}$ and $ATF3^{-/-}$ MEFs, respectively). As detected in HCT116 cells, ATF3 levels increased
141 in the $ATF3^{+/+}$ MEFs in response to IGG and PB exposure (Fig 2A). As expected, ATF3 was not
142 detected in the $ATF3^{-/-}$ MEFs. We assessed sensitivity to apoptosis by one parameter flow
143 cytometric analysis of sub G_1 DNA content in both cell lines following exposure to IGG and PB
144 (Fig. 2B). Cells deleted of ATF3 were significantly protected against the lethal affects of both
145 drugs. Therefore, PB and IGG appear to induce ATF3-dependent apoptosis in MEFs.
146

147 **Fig 2. ATF3 is activated in response to IGG and PB treatment in MEFs.** $ATF3^{+/+}$ and $ATF3^{-}$
148 $^{/-}$ MEFs were left untreated, or exposed to DMSO, 30μM IGG or 25nM PB for 24 hours. Protein
149 lysates were collected in 1% SDS and analyzed using immunoblot with the indicated antibodies
150 (A). MagicMark™ Western Protein Standard was used, the 30kDa and 40kDa marker are visible
151 on ATF3 and actin westerns, respectively. Similar results were obtained across three independent
152 experiments. Flow cytometric analysis of sub G_1 content was completed as described previously
153 for both $ATF3^{+/+}$ and $ATF3^{-/-}$ cells (B). A two-way ANOVA was completed comparing cell lines
154 and treatments, both having $p<0.001$.
155

156 The sensitivity of MEFs to spliceosome inhibition was further evaluated with two
157 additional independent assays. First, ATF3$^{+/+}$ and ATF3$^{-/-}$ MEFs were exposed to either IGG or
158 PB for 24h and cell viability was assessed by trypan blue dye exclusion (Fig 3A). Trypan blue is
159 unable to penetrate viable cells with intact cell membranes, whereas non-viable cells that have
160 lost membrane integrity take up the dye. Both splicing inhibitors (PB and IGG) decreased cell
161 viability in ATF3$^{+/+}$ MEFs. The surviving fractions of ATF3$^{-/-}$ MEFs was significantly higher
162 than parental controls following exposure to both drugs. In fact, there was no detectable decrease
163 in viability in the ATF3$^{-/-}$ MEFs with this assay.
164
165 **Fig 3. The absence of ATF3 increases cell viability following PB and IGG treatment**.
166 ATF3$^{+/+}$ MEFs (white) and ATF3$^{-/-}$ MEFs (grey) were incubated with 30μM IGG, 25nM PB and
167 200nM act D for 48h (A) or 24h (B). A trypan blue exclusion assay was used to assess
168 membrane integrity, as an indictor of cell viability (A). The CellTiter-Glo® Luminescent Cell
169 Viability Assay was used to estimate metabolic activity as an indicator of cell viability (B). Each
170 bar represents the mean of 3 independent experiments, +/- SEM. Statistical significance between
171 cell lines for each treatment was completed using a two-way ANOVA, with the comparison of
172 cell lines and treatments having $p<0.0001$.
173
174 Second, a CellTiter-Glo® Luminescent Cell Viability Assay was used to quantify ATP
175 levels in treated and untreated cells. A decrease in ATP in treated compared to untreated cells is
176 indicative of a decrease in the number of metabolically active cells (Fig 3B). ATP levels
177 decreased in both ATF3$^{+/+}$ and ATF3$^{-/-}$ MEFs following treatment with IGG and PB, consistent
178 with previous literature showing that both IGG and PB decreased cell viability [5, 6].

179 Importantly, the surviving fraction of treated ATF3$^{-/-}$ MEFs was significantly greater than the
180 surviving fraction of control MEFs suggesting that ATF3$^{-/-}$ MEFs were again protected from the
181 cytotoxic effects of both PB and IGG. Taken together, ATF3 expressing MEFs are more
182 sensitive to splicing inhibitors than their ATF3$^{-/-}$ counterparts, as assed by DNA fragmentation,
183 membrane integrity and ATP content.
184

185 # Discussion

186 The production of functional mRNAs requires the synthesis of pre-mRNA that is
187 coordinated with co-transcriptional mRNA processing steps including pre-mRNA splicing [13-
188 15]. The inhibition of pre-mRNA splicing delays or prevents the production of functional
189 mRNAs and indirectly the encoded proteins. How splicing abnormalities are sensed and
190 transmitted to cell death pathways remains unclear. In the present work, we measured cellular
191 responses to two spliceosome inhibitors, IGG and PB. We found that both drugs led to an
192 increase in ATF3 expression in human colon cancer cells and MEFs. Parental MEFs, expressing
193 ATF3, were sensitive to both inhibitors leading to a large decrease in the viable cell population.
194 However, cell viability was significantly higher in ATF3-/-, as assessed in 3 independent assays.
195 Subtle quantitative differences were detected among the assays that reflect the timing of
196 individual assays, the timing of changes associated with cell death and the sensitivity of
197 individual assays. Of note, CellTiter-Glo® Luminescent Cell Viability Assay is not determined
198 on a single cell basis and it is very sensitive [16] so it isn't entirely surprising that we detected
199 greater apparent cell death with this assay. Despite these differences, all three assays suggest that
200 ATF3 as a regulator of mammalian cell sensitivity to these pre-mRNA splicing inhibitors.

201 The two spliceosome inhibitors tested target distinct pre-spliceosome complexes. PB
202 interacts with the SF3B1 subunit of the U2 snRNP in the complex A [5] whereas IGG acts
203 somewhat later preventing the transition from the A to B complex through an unknown target
204 [4]. Despite the fact that both drugs inhibit pre-mRNA splicing at similar stages and induce
205 apoptosis through an ATF3-dependent mechanism, a variety of differences in gene expression
206 and biological effects have been described. For example, we have previously reported that these
207 two drugs can have pronounced effects on cell cycle distribution [17]. Importantly, these drugs
208 led to similar but not identical changes in cell cycle distribution [17]. Two parameter flow
209 cytometric analysis of bromodeoxyuridine-labelled cells indicated that IGG led to multiple cell
210 cycle alterations but the most prominent was to an S phase arrest [17]. In partial contrast, PB-
211 treated cells were blocked predominantly in G_1 but also exhibited a more modest S phase arrest
212 than IGG-treated cells [17]. Meanwhile, both drugs led to decreased M phase assessed by loss of
213 phospho-H3 immunoreactivity [17]. Therefore, there are similarities and differences in the
214 effects of these compounds on cell cycle responses.
215 Other groups have reported recently that IGG has other unique effects on transcription
216 and protein trafficking. Boswell and coworkers found that IGG decreases transcriptional
217 elongation, independent of effects on pre-mRNA splicing [18]. Strand-specific RNA-sequencing
218 (RNA-seq) was performed in IGG-treated and control cells and relative read number increased
219 within 5 kb of transcription start sites in IGG-treated cells but not in the presence of an SF3B1
220 inhibitor, meayamycin [19], suggesting that transcription near the 5'end of genes was slow in the
221 presence of IGG [18]. These authors also detected increased polyA site readthrough in IGG
222 treated cells further suggesting that a fundamental problem in transcription and co-transcriptional
223 processing may underlie some of the unique biological effects of IGG [18]. It is noteworthy that

224 these authors still detected a defect in pre-mRNA splicing using RNA-seq analysis in this and
225 previous papers [18, 20].
226 Lastly, IGG also appear to inhibit trafficking of the amyloid precursor protein (APP)
227 from endoplasmic reticulum (ER) to the Golgi [21] and lysosome-mediated turnover [22]. In the
228 former, APP levels increased in response to IGG but not the SF3B1 inhibitor spliceostatin [21].
229 APP was retained in the ER and where the protein was stable and accumulated [21]. In the latter
230 paper [22], IGG led to increased lysosomal stress, increased TFEB protein expression (a
231 regulator of lysosomal biogenesis) and the accumulation of polyubiquitinated proteins under
232 nutrient starving conditions suggesting that IGG may be inhibiting proteasomes and altering
233 lysosomal function under some conditions [22]. Intriguingly, IGG-induced TFEB activated
234 ATF3 indirectly through ATF4, however it was unclear if ATF3 contributed to cell death
235 detected in this manuscript. There is presently no evidence that PB or any other SF3B1 inhibitors
236 similarly affect protein homeostasis. While these additional functions attributed to IGG may
237 contribute to differences detected in cell cycle regulation [17] yet they don't appear to grossly
238 alter the ATF3-dependence of cell death induced by IGG and PB. It is likely that IGG and PB
239 lead to ATF3 induction through a common mechanism related to spliceosome inhibition.
240

241 # Conclusions

242 ATF3 is involved in a variety of stress pathways, and it is likely that a disruption in
243 spliceosome formation is leading to activation of ATF3, in turn promoting apoptosis. The novel
244 findings here provide evidence that splicing inhibitors lead to activation of ATF3, and that
245 ATF3, in turn, is playing a role in determining sensitivity of cells to these compounds. Our future

work will investigate the role ATF3 has on cell sensitivity, and work to determine how each of these splicing inhibitors specifically led to ATF3 activation.

Acknowledgements

We would like to thank Dr. Jim Dimitroulakos (Princess Margaret Research Institute, Toronto, ON) for providing mouse embryonic fibroblasts.

References

1. Hoskins AA, Moore MJ. The spliceosome: a flexible, reversible macromolecular machine. Trends Biochem Sci. 2012;37(5):179-88. doi: 10.1016/j.tibs.2012.02.009. PubMed PMID: 22480731; PubMed Central PMCID: PMCPMC3508674.
2. Jurica MS, Moore MJ. Pre-mRNA splicing: awash in a sea of proteins. Molecular cell. 2003;12(1):5-14. doi: 10.1016/s1097-2765(03)00270-3. PubMed PMID: 12887888.
3. Kotake Y, Sagane K, Owa T, Mimori-Kiyosue Y, Shimizu H, Uesugi M, et al. Splicing factor SF3b as a target of the antitumor natural product pladienolide. Nature chemical biology. 2007;3(9):570-5. PubMed PMID: 17643112.
4. O'Brien K, Matlin AJ, Lowell AM, Moore MJ. The biflavonoid isoginkgetin is a general inhibitor of Pre-mRNA splicing. The Journal of biological chemistry. 2008;283(48):33147-54. PubMed PMID: 18826947.
5. Yokoi A, Kotake Y, Takahashi K, Kadowaki T, Matsumoto Y, Minoshima Y, et al. Biological validation that SF3b is a target of the antitumor macrolide pladienolide. FEBS J. 2011;278(24):4870-80. doi: 10.1111/j.1742-4658.2011.08387.x. PubMed PMID: 21981285.
6. Yoon SO, Shin S, Lee HJ, Chun HK, Chung AS. Isoginkgetin inhibits tumor cell invasion by regulating phosphatidylinositol 3-kinase/Akt-dependent matrix metalloproteinase-9 expression. Molecular cancer therapeutics. 2006;5(11):2666-75. PubMed PMID: 17121913.
7. Fan F, Jin S, Amundson SA, Tong T, Fan W, Zhao H, et al. ATF3 induction following DNA damage is regulated by distinct signaling pathways and over-expression of ATF3 protein suppresses cells growth. Oncogene. 2002;21(49):7488-96. doi: 10.1038/sj.onc.1205896. PubMed PMID: 12386811.
8. Gurzov EN, Barthson J, Marhfour I, Ortis F, Naamane N, Igoillo-Esteve M, et al. Pancreatic beta-cells activate a JunB/ATF3-dependent survival pathway during inflammation. Oncogene. 2012;31(13):1723-32. doi: 10.1038/onc.2011.353. PubMed PMID: 21841823.
9. Schroder M, Kaufman RJ. ER stress and the unfolded protein response. Mutation research. 2005;569(1-2):29-63. doi: 10.1016/j.mrfmmm.2004.06.056. PubMed PMID: 15603751.
10. Fels DR, Koumenis C. The PERK/eIF2alpha/ATF4 module of the UPR in hypoxia resistance and tumor growth. Cancer Biol Ther. 2006;5(7):723-8. doi: 10.4161/cbt.5.7.2967. PubMed PMID: 16861899.
11. Thompson MR, Xu D, Williams BR. ATF3 transcription factor and its emerging roles in immunity and cancer. J Mol Med (Berl). 2009;87(11):1053-60. doi: 10.1007/s00109-009-0520-x. PubMed PMID: 19705082; PubMed Central PMCID: PMCPMC2783469.

284 12. Mungrue IN, Pagnon J, Kohannim O, Gargalovic PS, Lusis AJ. CHAC1/MGC4504 is a novel
285 proapoptotic component of the unfolded protein response, downstream of the ATF4-ATF3-CHOP
286 cascade. J Immunol. 2009;182(1):466-76. PubMed PMID: 19109178; PubMed Central PMCID:
287 PMCPMC2846782.
288 13. Saldi T, Cortazar MA, Sheridan RM, Bentley DL. Coupling of RNA Polymerase II Transcription
289 Elongation with Pre-mRNA Splicing. J Mol Biol. 2016;428(12):2623-35. doi: 10.1016/j.jmb.2016.04.017.
290 PubMed PMID: 27107644; PubMed Central PMCID: PMCPMC4893998.
291 14. Carmo-Fonseca M, Kirchhausen T. The timing of pre-mRNA splicing visualized in real-time.
292 Nucleus. 2014;5(1):11-4. doi: 10.4161/nucl.28056. PubMed PMID: 24637398; PubMed Central PMCID:
293 PMCPMC4028348.
294 15. Lee KM, Tarn WY. Coupling pre-mRNA processing to transcription on the RNA factory assembly
295 line. RNA Biol. 2013;10(3):380-90. doi: 10.4161/rna.23697. PubMed PMID: 23392244; PubMed Central
296 PMCID: PMCPMC3672281.
297 16. Nowak E, Kammerer S, Kupper JH. ATP-based cell viability assay is superior to trypan blue
298 exclusion and XTT assay in measuring cytotoxicity of anticancer drugs Taxol and Imatinib, and
299 proteasome inhibitor MG-132 on human hepatoma cell line HepG2. Clin Hemorheol Microcirc.
300 2018;69(1-2):327-36. doi: 10.3233/CH-189120. PubMed PMID: 29630545.
301 17. Vanzyl EJ, Rick KRC, Blackmore AB, MacFarlane EM, McKay BC. Flow cytometric analysis
302 identifies changes in S and M phases as novel cell cycle alterations induced by the splicing inhibitor
303 isoginkgetin. PLoS One. 2018;13(1):e0191178. doi: 10.1371/journal.pone.0191178. PubMed PMID:
304 29338026; PubMed Central PMCID: PMCPMC5770052.
305 18. Boswell SA, Snavely A, Landry HM, Churchman LS, Gray JM, Springer M. Total RNA-seq to
306 identify pharmacological effects on specific stages of mRNA synthesis. Nature chemical biology.
307 2017;13(5):501-7. doi: 10.1038/nchembio.2317. PubMed PMID: 28263964.
308 19. Albert BJ, McPherson PA, O'Brien K, Czaicki NL, Destefino V, Osman S, et al. Meayamycin inhibits
309 pre-messenger RNA splicing and exhibits picomolar activity against multidrug-resistant cells. Molecular
310 cancer therapeutics. 2009;8(8):2308-18. PubMed PMID: 19671752.
311 20. Gray JM, Harmin DA, Boswell SA, Cloonan N, Mullen TE, Ling JJ, et al. SnapShot-Seq: a method
312 for extracting genome-wide, in vivo mRNA dynamics from a single total RNA sample. PLoS One.
313 2014;9(2):e89673. doi: 10.1371/journal.pone.0089673. PubMed PMID: 24586954; PubMed Central
314 PMCID: PMCPMC3935918.
315 21. Bai B, Wang S, Chen Y, Jia J, Tian X, Liu C, et al. Effects of RNA Splicing Inhibitors on Amyloid
316 Precursor Protein Expression. ACS Omega. 2018;3(3):2798-803. doi: 10.1021/acsomega.7b02073.
317 PubMed PMID: 30221221; PubMed Central PMCID: PMCPMC6130791.
318 22. Tsalikis J, Abdel-Nour M, Farahvash A, Sorbara MT, Poon S, Philpott DJ, et al. Isoginkgetin, a
319 Natural Biflavonoid Proteasome Inhibitor, Sensitizes Cancer Cells to Apoptosis via Disruption of
320 Lysosomal Homeostasis and Impaired Protein Clearance. Molecular and cellular biology. 2019;39(10).
321 doi: 10.1128/MCB.00489-18. PubMed PMID: 30910794; PubMed Central PMCID: PMCPMC6497994.

322

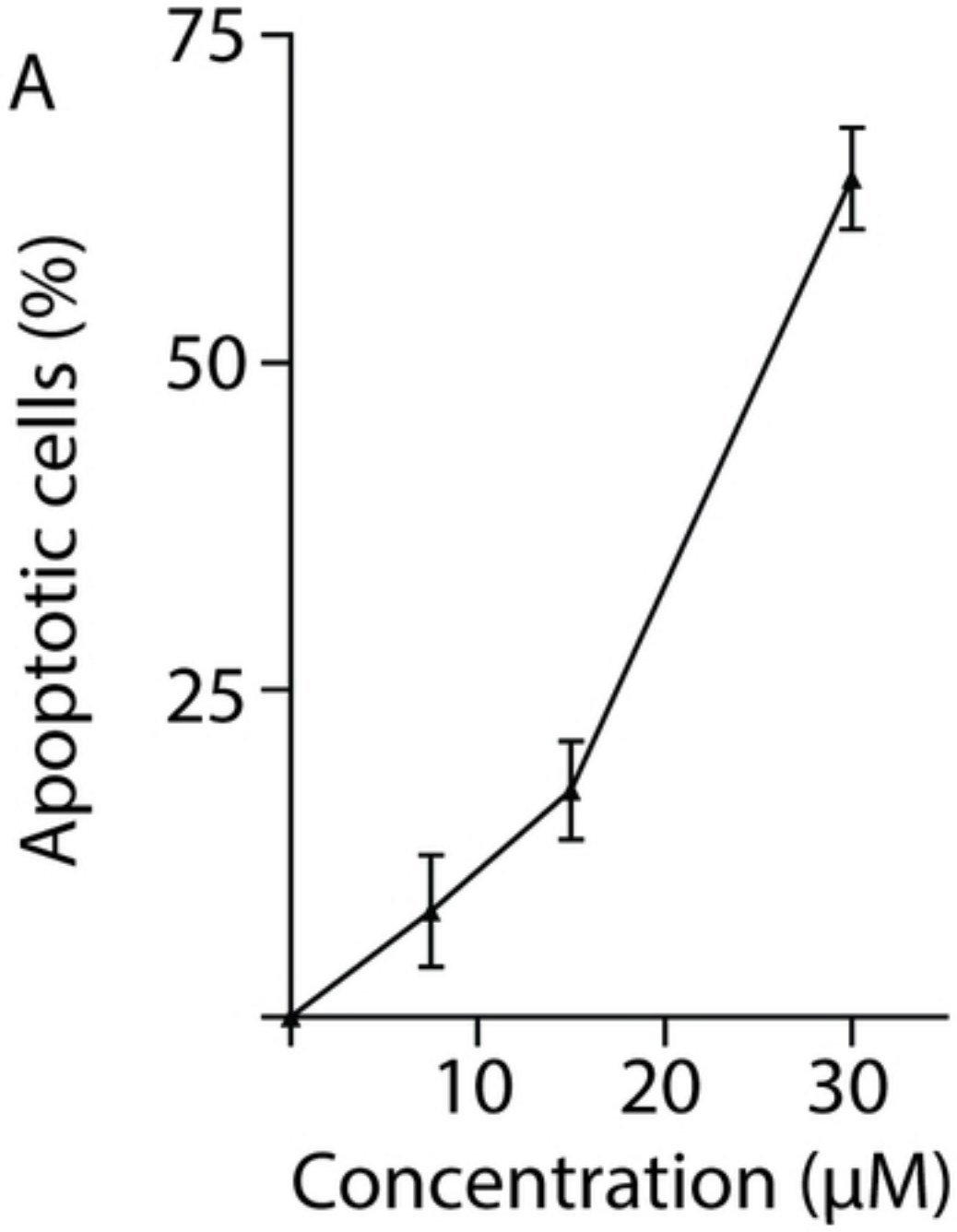
A
75
50
25
Apoptotic cells (%)
10
20
30
Concentration (μM)

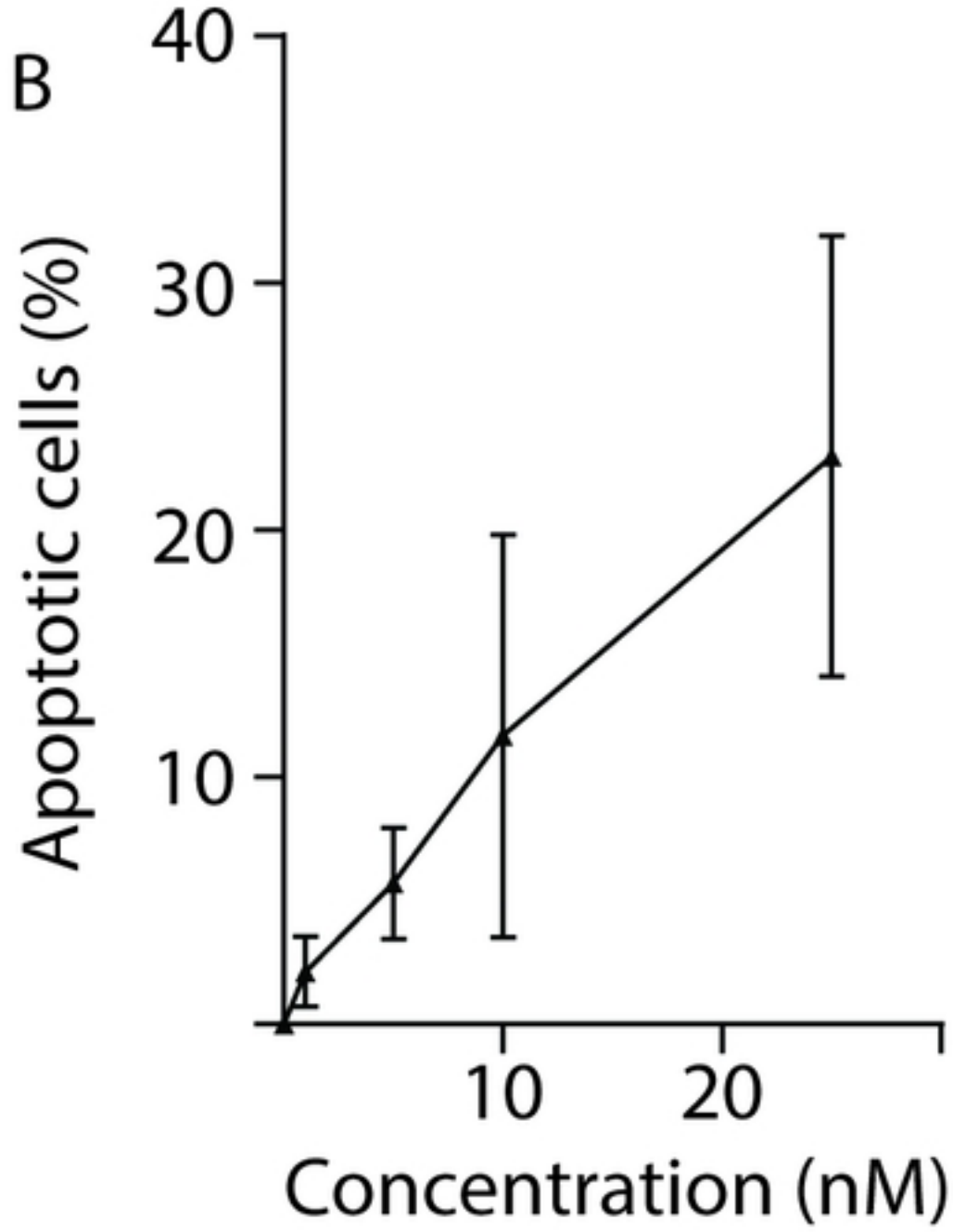
B
40
30
20
10
Apoptotic cells (%)
10
20
Concentration (nM)

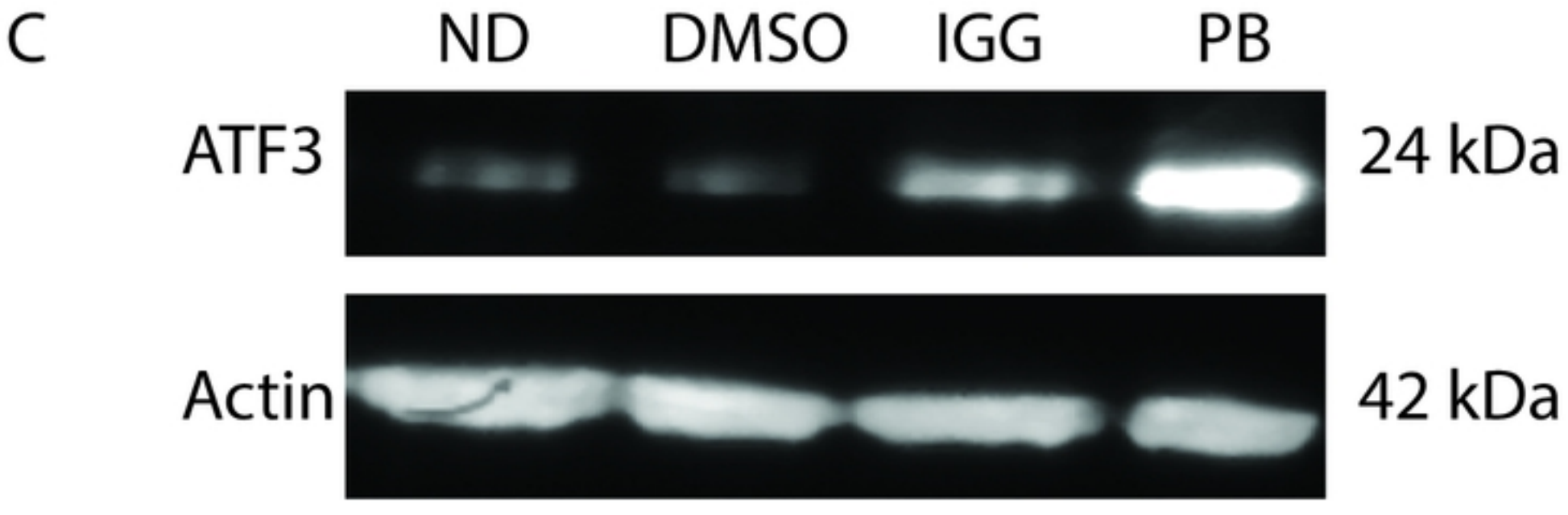
C
ND
DMSO
IGG
PB
ATF3
24 kDa
Actin
42 kDa

Figure 1

A

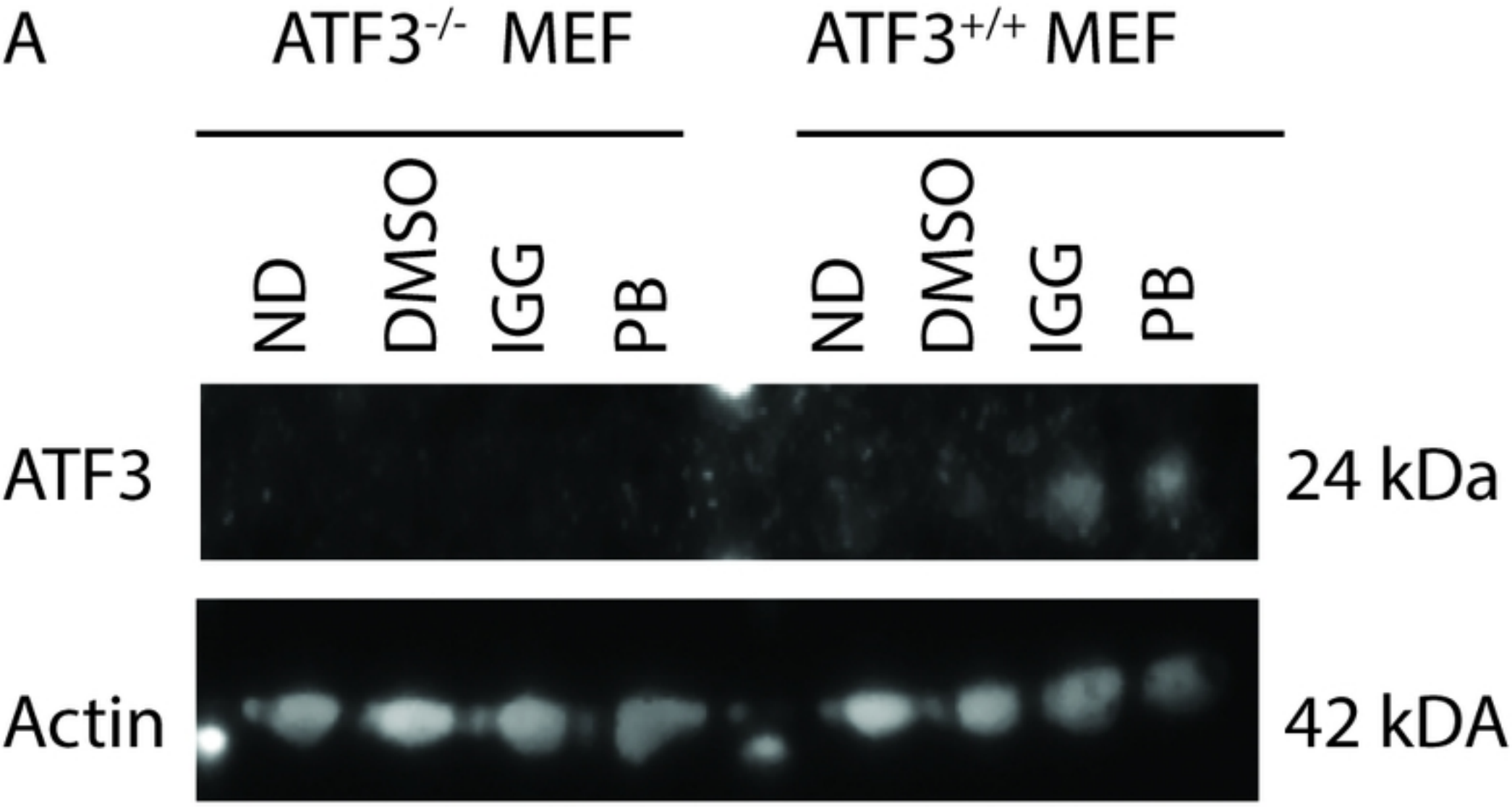
ATF3-/- MEF
ATF3+/+ MEF
ND
DMSO
IGG
PB
ND
DMSO
IGG
PB
ATF3
24 kDa
Actin
42 kDA

B

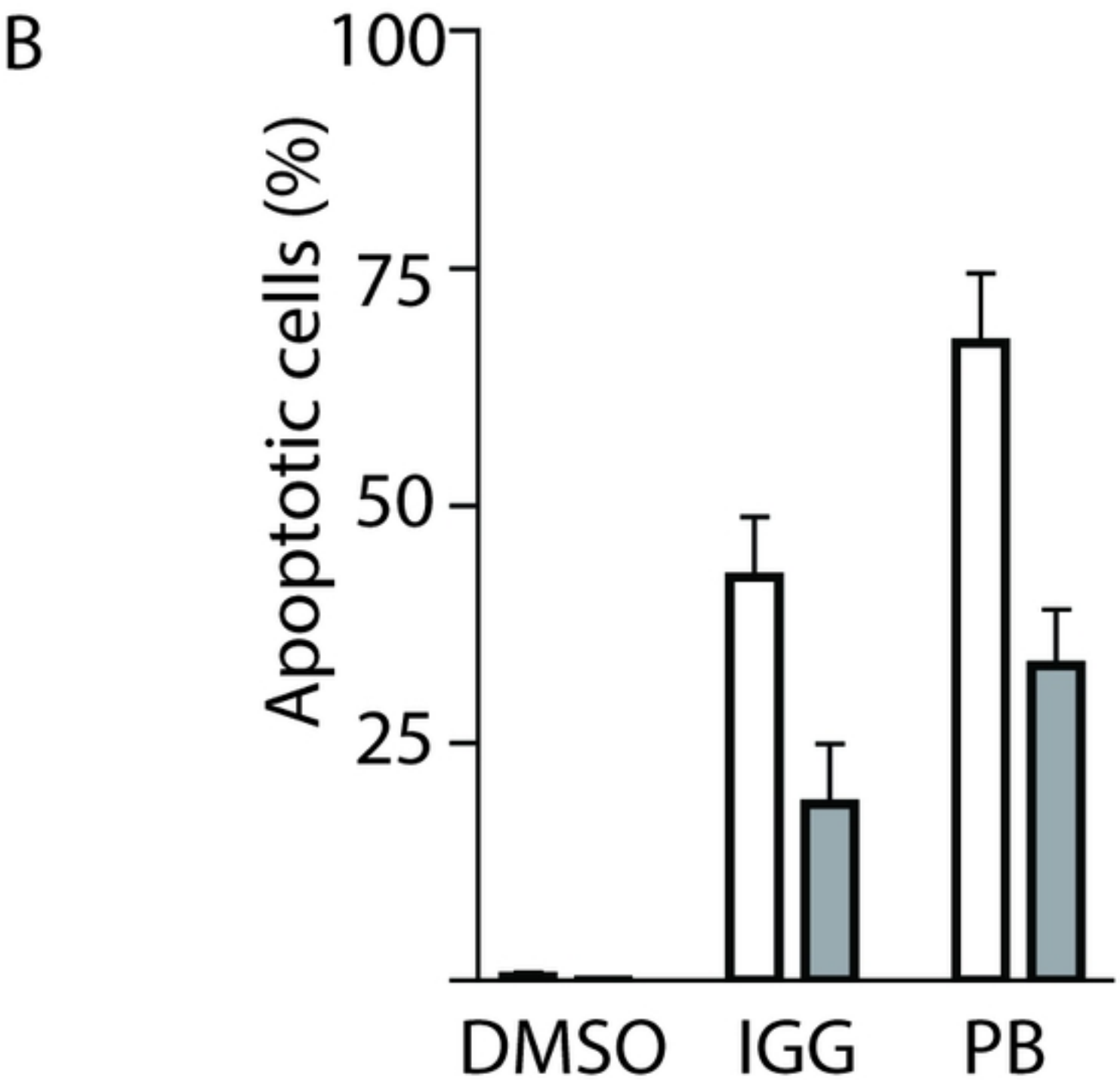
Apoptotic cells (%)
100
75
50
25
DMSO
IGG
PB

Figure 2

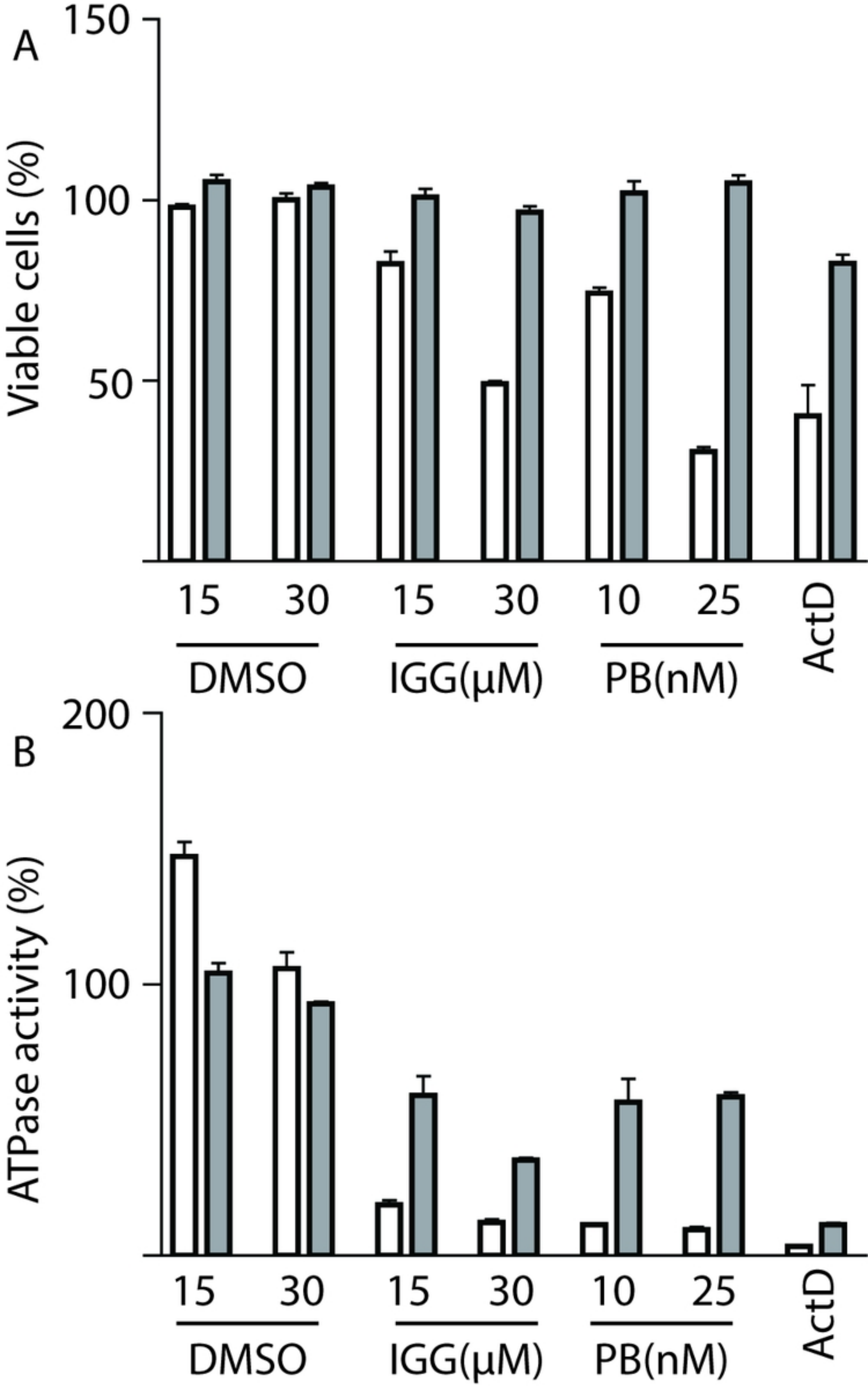
A
Viable cells (%)
150
100
50
15
30
15
30
10
25
ActD
DMSO
IGG(μM)
PB(nM)
B
ATPase activity (%)
200
100
15
30
15
30
10
25
ActD
DMSO
IGG(μM)
PB(nM)

Figure 3